

SIMULATION SOFTWARE TO DESCRIBE THE THERMAL ENVIRONMENT OF RESIDENTIAL BUILDINGS BASED ON DETAILED PHYSICAL MODELS

Akihito Ozaki*, Toshiyuki Watanabe**, Shigeki Iwaoka*** and Shuho Takase**

* The University of Kitakyushu, Fukuoka, Japan

** Kyushu University, Fukuoka, Japan

***ATOM Indoor Climate Institute, Morioka, Japan

ozaki@env.kitakyu-u.ac.jp

ABSTRACT

A simulation software called THERB has been developed for the purpose of estimating the thermal environment of residential buildings. THERB can simulate dynamic fluctuation of temperature, humidity, sensible temperature such as PMV or SET* (Predicted Mean Vote or Standard Effective Temperature) and heating/cooling load by taking into account both the air temperature and the sensible temperature for multiple zone buildings. The heat transfer models used in THERB such as conduction, convection, radiation and ventilation (or air leakage) are based upon the detailed phenomena describing actual building physics. All the phenomena are calculated without simplification of the heat transfer principles of any building component or element. The paper describes the detailed models used in THERB, and prominent features of the models are explained in detail.

INTRODUCTION

THERB (the simulation software of the thermal environment of residential buildings) is a dynamic simulation software which can estimate temperature, humidity, sensible temperature, and heating/cooling load for multiple zone buildings. The model can be applied to all forms of building design, structure or occupant schedules, etc. The following outlines the algorithms for heat transfer used in THERB, which are derived from fundamental building physics principles.

Conductive Heat Transfer: The successive transition method [1], which is based on a state equation in the modern control theory, is applied to the model of one-dimensional transient thermal conduction of multi-layer walls in the time-discrete domain. One of the principle advantages of the successive transition method compared to the numerical convolution method represented by the response factor [2] are that the successive transition method requires only an input excitation at one time step before from the present time step. An additional advantage of the successive

transition method is that the calculation time and storage capacity depends only on the number of exponential terms of the characteristic function. One can take advantage of the superior feature of the successive transition method by making use of a revised four terminals determinant which can dramatically decrease the number of exponential terms [3],[4], the calculation time and storage capacity. Regarding thermal conduction to the ground, the finite difference method is applied to the previous calculation of the ground temperature and then the results are used as the input excitation for conductive calculation of the earthen floor and basement walls by the successive transition method using input data of the building described in THERB. Furthermore, the successive transition method used in THERB utilizes a trapezoid wave instead of an isosceles triangle wave which is easily adaptable to a hold function. This can significantly improve the calculation accuracy of conductive heat because one can adjust the hold function to the time-discrete domain.

Convective Heat Transfer: By default, the convective heat transfer coefficients in THERB are recalculated at every time step on all surfaces of the exterior, interior and cavities of buildings using dimensionless equations which are derived from either the profile method for boundary layer [5] (based on the energy equation, the momentum equation and the fluid friction) or defined from the experimental findings according to natural or forced convection [6],[7]. Furthermore the natural convective heat transfer coefficients are classified into either vertical or horizontal surfaces. It is possible to use the functional equations of the wind direction and velocity for the exterior convective heat transfer coefficients and the functional equations of the temperature difference between surface and room for the interior convective heat transfer coefficients. It is also possible to set constant all day long or during air-conditioning time by every part of the buildings.

Radiant Heat Transfer: On the exterior surfaces of the buildings, the standard method of using the radiant heat transfer coefficients and atmospheric radiation is applied. On the interior of buildings, instead of the general method (that is, the calculation of heat transfer between surface and indoor air and radiation between surfaces), the use of the long-wave absorption coefficient makes possible to simulate a net absorption of radiant heat as a consequence of multiplex reflection among interior surfaces. Mutual radiation between the surfaces of cavities in walls and windows can be also simulated.

Incident Solar Radiation: Incident solar radiation on the exterior and into the interior of buildings is divided into direct and diffuse solar radiation and calculated for all parts of the building in all directions using accurate geometric calculations of shaded and unshaded portions of the building by considering the influence of overhangs and wings. Isotropic model or anisotropic [8] models can be chosen for diffused solar radiation. Transmitted solar radiation is calculated by the multi-layer window model [9] and considers multiplex reflection (depending on an incidence angle of solar radiation) between not only the glazing layers but also between the window and interior shade at every time step. The multiplex reflection of both direct and diffuse solar radiation among interior surfaces including re-transmission of solar radiation from the inside to the outside through the windows is simulated by using the short-wave absorption coefficient. Moreover the absorption coefficients of long and short wave are applied to radiant heat emitted from lights and appliances, etc.

Ventilation: The network airflow model integrating a thermal model with a plant model estimates natural and forced ventilation quantities of each zone (rooms and cavities) caused by air leakage, infiltration and mechanical ventilation. As for independent ventilated cavities in the walls, it is possible to estimate airflow quantities by hydrodynamic analysis as the solution to the equations of motion, energy and continuity [10]. Constant ventilation quantities can be also set every hour for all zones.

Control of space conditioning: Control methods for space conditioning are classified into three types of heating, cooling, and simultaneous heating and cooling. By default, humidity control and temperature control are linked. Temperature and humidity setpoint and ranges can be optionally set every hour. Moreover the control of humidity is automatically performed in case the sensible temperature is set as the setpoint of air-conditioning.

THEORETICAL FEATURE OF THERB CONDUCTION

The numerical convolution method represented by the response factor method or the transfer function method [11] is well known as a calculation method for transient thermal conduction in the time-discrete domain. The biggest disadvantage of this method is all the past input excitation, which influences the present conductive heat, is required. Thus in the case of walls with large thermal capacity, large calculation time and storage capacity are required. To overcome this problem of the numerical convolution method, the successive transition method is used in THERB. The equations for the successive transition method can be developed from the pulse transfer function with the fundamental wave of input excitation by using the z transformation if it is assumed the characteristic function of multi-layer walls is already known.

Characteristic Function

Unit response $\phi(t)$ of the heat flux on a surface of multi-layer wall with temperature excitation of the surface (or air) is generally expressed by Eq.(1).

$$\phi(t) = A_0 + \sum_{k=1}^{\infty} A_k e^{-\alpha_k t} \quad (1)$$

A_0 is the thermal conductance (or overall coefficient of heat transfer). The maximum value of k cannot be equal to infinity, thus k is broken off K_0 and Eq.(1) is arranged into Eq.(2).

$$\phi(t) = A_0 + \sum_{k=1}^{K_0} A_k e^{-\alpha_k t} + \dot{Q} \delta(t) \quad (2)$$

$\delta(t)$ is Dirac's function. \dot{Q} is the moment heat flux at $t=0^+$ and expressed as follows:

$$\dot{Q} = \sum_{k=K_0+1}^{\infty} \frac{A_k}{\alpha_k} \quad (3)$$

The transfer function $G(s)$ is obtained as the product of the Laplace transformation of $\phi(t)$ and s .

$$G(s) = A_0 + \sum_{k=1}^{K_0} \frac{A_k s}{s + \alpha_k} + \dot{Q} s \quad (4)$$

Hold Function

The following equations are the Laplace transformation of the hold function $G_h(s)$ using a trapezoid wave to approximate time-discrete input excitation. As shown in Fig.1, the trapezoid hold functions are composed of right angle triangles.

$$G_{ht}(s) = \left(\frac{1 - e^{-st}}{s} \right) + h \left(-\frac{e^{-st}}{s} + \frac{1 - e^{-st}}{Ts^2} \right) \quad (5)$$

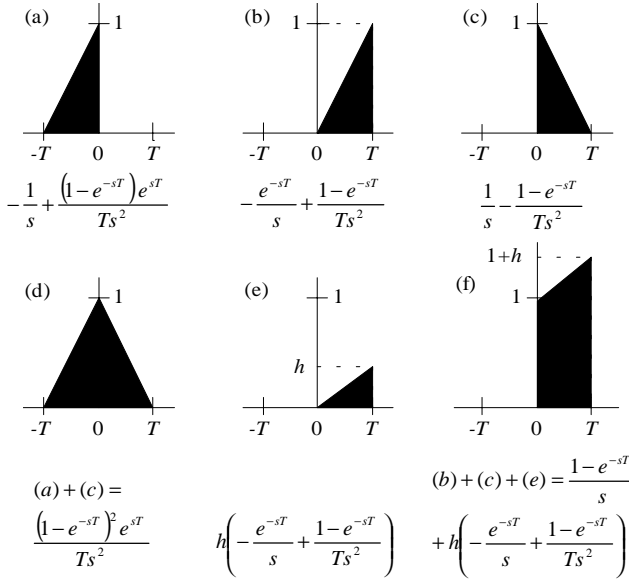


Fig.1 Composition of the trapezoid hold function

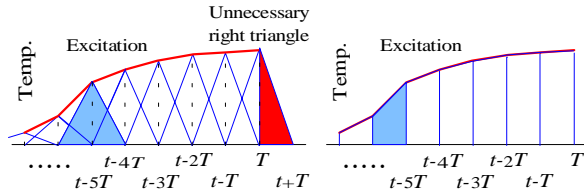


Fig.2 Adjustment of hold function to time discrete domain

The trapezoid hold function has the advantage over the isosceles triangle hold function in that it can adjust itself to the time-discrete domains as in Fig.2.

Pulse Transfer Function

The pulse transfer function $G(z)$ is defined as the z transformation of the product of the transfer function $G(s)$ and the hold function $G_h(s)$ [12].

$$G(z) = Z\{G(s) \cdot G_h(s)\} \quad (6)$$

The pulse transfer function $G_t(z)$ with the trapezoid hold functions $G_{ht}(s)$ are obtained by Eq.(7).

$$G_t(z) = A_0 + \sum_{k=1}^{K_0} \frac{A_k(1-z^{-1})}{1-e^{-\alpha_k T} z^{-1}} + h \sum_{k=1}^{K_0} \frac{A_k(1-e^{-\alpha_k T} - \alpha_k T)}{\alpha_k T} \cdot \frac{z^{-1}}{1-e^{-\alpha_k T} z^{-1}} + \frac{\dot{Q}}{T}(1-z^{-1}) \quad (7)$$

where the z transformation of the differentiation of $G_{ht}(s)$ becomes $(1-z^{-1})/T$ [13].

Relation between Input and Output Parameters

The relation between input and output parameters is expressed by Eq.(8) using the pulse transfer function $G(z)$.

$$Q(z) = G(z) \cdot \Theta(z) \quad (8)$$

$\Theta(z)$ and $Q(z)$ are the z transformation of impulse data of the input $\theta(t)$ and the output $q(t)$, and are described by Eqs.(9), (10) for the case when the time-discrete values of the input and output are θ_n and q_n at $t=nT$ (T is an interval of time), respectively.

$$\Theta(z) = \theta_0 + \theta_1 z^{-1} + \theta_2 z^{-2} + \dots \quad (9)$$

$$Q(z) = q_0 + q_1 z^{-1} + q_2 z^{-2} + \dots \quad (10)$$

Successive Transition Method

The state transition function $X_k(z)$ with the trapezoid pulse transfer function is defined by Eq.(11) as the product of the right side second and third terms of Eq.(7) and the time-discrete input $\Theta(z)$.

$$X_k(z) = \left\{ \frac{A_k(1-z^{-1})}{1-e^{-\alpha_k T} z^{-1}} + h \frac{A_k(1-e^{-\alpha_k T} - \alpha_k T)}{\alpha_k T} \cdot \frac{z^{-1}}{1-e^{-\alpha_k T} z^{-1}} \right\} \Theta(z) \quad (11)$$

Eq.(11) can be re-arranged into Eq.(12).

$$(1-e^{-\alpha_k T} z^{-1})X_k(z) = \left\{ A_k(1-z^{-1}) + h \frac{A_k(1-e^{-\alpha_k T} - \alpha_k T)}{\alpha_k T} z^{-1} \right\} \Theta(z) \quad (12)$$

By substituting $X_k(z) = x_{k,0} + x_{k,1}z^{-1} + x_{k,2}z^{-2} + \dots$ and $\Theta(z) = \theta_0 + \theta_1 z^{-1} + \theta_2 z^{-2} + \dots$ in Eq.(12) and comparing the coefficients of z^{-n} on the left and right sides of the function in Eq.(12), the following state transition equation is obtained.

$$x_{k,n} = e^{-\alpha_k T} x_{k,n-1} + A_k(\theta_n - \theta_{n-1}) + h \frac{A_k(1-e^{-\alpha_k T} - \alpha_k T)}{\alpha_k T} \theta_{n-1} \quad (13)$$

The inclination parameter h is obtained by Eq.(14).

$$h\theta_{n-1} = \theta_n - \theta_{n-1} \quad (14)$$

Eq.(13) is rearranged to Eq.(15) by substituting Eq.(14).

$$x_{k,n} = e^{-\alpha_k T} x_{k,n-1} + \frac{A_k(1-e^{-\alpha_k T})}{\alpha_k T} (\theta_n - \theta_{n-1}) \quad (15)$$

where $x_{k,0} = A_k \theta_0$.

The right side of Eq.(8) can be expanded to an infinite series with respect to $x_{k,n}$ (the state transition function) by substituting Eqs.(7), (9) and (15). By comparing the coefficients of z^{-n} on the left and right sides of Eq.(8), the time-discrete output can be defined by Eq.(16).

$$q_n = A_0 \theta_n + \sum_{k=1}^{K_n} x_{k,n} + \frac{\dot{Q}}{T} (\theta_n - \theta_{n-1}) \quad (16)$$

Practical Formulas of Successive Transition Method

The followings are the formulas developed from Eq.(16), which express the net heat flux CD on surface \bar{j} taking into consideration the heat flux from the opposite surface j of wall at the present time n .

$$CD_{\bar{j},n} = a_j \theta_{\bar{j},n} - a_t \theta_{j,n} + D_{\bar{j},n-1} \quad (17)$$

$$\begin{aligned} \varphi_k &= e^{-\alpha_k T} \\ p_k &= \varphi_k - (1 - \varphi_k) / \alpha_k T \\ q_k &= -p_k - (1 - \varphi_k) \end{aligned} \quad (18)$$

$$a_m = A_0 + \sum_{k=1}^{K_0} A_{m,k} (1 + q_k) + \dot{Q}_m / T \quad (19)$$

$$b_m = \sum_{k=1}^{K_0} A_{m,k} p_k - \dot{Q}_m / T$$

$$D_{\bar{j},n-1} = \sum_{k=1}^{K_0} \varphi_k x_{\bar{j},k,n-1} + b_{\bar{j}} \theta_{\bar{j},n-1} - b_t \theta_{j,n-1} \quad (20)$$

$x_{\bar{j},k,n-1}$ of Eq.(20) is renewed by every time step by Eq.(21).

$$\begin{aligned} x_{\bar{j},k,n} &= \varphi_k x_{\bar{j},k,n-1} + p_k (A_{\bar{j},k} \theta_{\bar{j},n-1} - A_{r,k} \theta_{j,n-1}) \\ &\quad + q_k (A_{\bar{j},k} \theta_{\bar{j},n} - A_{r,k} \theta_{j,n}) \end{aligned} \quad (21)$$

where subscript $m = \bar{j}$ refers to the heat flux of the surface \bar{j} , and $m = t$ refers to the heat transmission through the surface j toward the surface \bar{j} .

CONVECTION

Table 1 shows the default of the convective heat transfer coefficients, which are developed on the basis of the profile method for boundary layer or experimental findings. THERB recalculates the coefficients by every time step on all surfaces of the exterior, interior and cavities of buildings.

Table 1 Convective Heat Transfer Coefficient

Part of Buildings	Dimensionless Number
Exterior	$Nu = 0.037 Re^{0.8} Pr^{1/3}$
Interior (Vertical Plane)	$Nu = 0.241 (Gr_i \cdot Pr)^{0.4}$ $Gr_i = g \beta \Delta T_a l^3 / \nu^2$
Interior (Horizontal Plane)	$Nu = C \cdot Ra_f^m$ $Ra_f = Gr_f \cdot Pr$ $f = (T_s + T_\infty) / 2$
Upward	$C=0.58, m=1/5$
Downward	$C=0.54, m=1/4$ ($Ra_f: 2E4$ to $8E6$) $C=0.15, m=1/3$ ($Ra_f: 8E6$ to $1E11$)
Cavity (ventilated)	$Nu = 0.023 Re^{0.8} Pr^{0.4}$

Cavity (closed)	$Nu = 0.035 (Gr_c \cdot Pr)^{0.38}$ $Gr_c = g \Delta T_s l^3 / T_m \nu^2$
-----------------	--

Gr : Grashof number, Nu : Nusselt number, Pr : Prandtl number, Ra : Rayleigh number, T_m : mean temperature of surfaces, ΔT_a : temperature difference between surface and air, ΔT_s : temperature difference between surfaces, g : gravitational constant, l : length, β : expansion coefficient, ν : kinematic viscosity

RADIATION

Multiplex Reflection of Long-Wave Radiation

The multiplex reflection of long-wave radiation between interior surfaces is simulated on the basis of Gebhart's absorption coefficient [14]. The long-wave absorption coefficient $\beta_{l,j}$ is defined as the net ratio of absorbed radiant heat on surface j from the surface l .

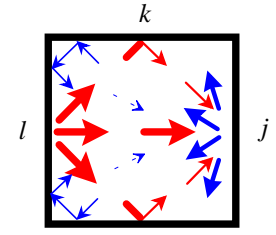


Fig.3 multiple reflection of long-wave radiation

$$\beta_{l,j} = F_{l,j} \varepsilon_j + \sum_{k=1}^J F_{l,k} (1 - \varepsilon_k) \beta_{k,j} \quad (22)$$

where $F_{l,j}$ is the view factor from the surface l to the surface j and ε_j is emissivity of the surface j .

Thus the net radiant heat emitted from the surface j (see Fig.3) is expressed by Eq.(23).

$$ELR_j = \varepsilon_j \sigma T_j^4 - \sum_{k=1}^J \beta_{k,j} \varepsilon_k \sigma T_k^4 S_k / S_j \quad (23)$$

Eq.(23) can be re-arranged into Eq.(25) by using the principle of the conservation of energy and the reciprocal theorem expressed by Eq.(24).

$$\sum_{k=1}^J \beta_{j,k} = 1 \quad (24)$$

$$\varepsilon_k S_k \beta_{k,j} = \varepsilon_j S_j \beta_{j,k}$$

$$\begin{aligned} ELR_j &= \varepsilon_j \sigma \sum_{k=1}^J \beta_{j,k} (T_j^4 - T_k^4) \\ &= \sum_{k=1}^J \beta_{j,k} \alpha_{r,jk} (T_j - T_k) \end{aligned} \quad (25)$$

where S_j is the area of surface j . $\alpha_{r,jk}$ is the radiant heat transfer coefficient from surface j to surface k and can be approximated by Eq.(26).

$$\alpha_{r,jk} \equiv 4 \varepsilon_j \sigma \left\{ (T_j + T_k) / 2 \right\}^3 \quad (26)$$

The long-wave absorption coefficient can be applied to long-wave radiant heat emitted from lights and appliances and human bodies, etc. If it is assumed that such radiant heat is equally emitted from the ceiling or

floor, the absorption amount ALR_j on the surface j can be described by Eq.(27).

$$ALR_j = \sum_{c=1}^C \beta_{c,j} LI_c S_c / S_j + \sum_{f=1}^F \beta_{f,j} LH_f S_f / S_j$$

$$= \varepsilon_j \left(\sum_{c=1}^C \beta_{j,c} LI_c / \varepsilon_c + \sum_{f=1}^F \beta_{j,f} LH_f / \varepsilon_f \right) \quad (27)$$

where LI_c and LH_f are the radiant heat from lights and appliances and human bodies, respectively. Thus the net radiant heat emitted from the surface j can be calculated by Eq.(28).

$$NLR_j = ELR_j - ALR_j \quad (28)$$

Multiplex Reflection of Short-Wave Radiation

Regarding direct solar radiation, when TDN_m is the transmitted direct solar radiation through the window striking a normal surface m , a_l and ρ_l are the solar absorptance and reflectance on the surface l , θ_l is incidence angle upon the interior surface l , and S_l is the insolation area of the surface l . The solar absorption and reflection on the surface l are expressed by $a_l \cdot TDN_m \cos \theta_l$ and $\rho_l \cdot TDN_m \cos \theta_l$, respectively. Solar absorption $ADT_{m,j}$ on the surface j based on TDN_m is expressed as Eq.(30) by using the short-wave absorption coefficient $\gamma_{l,j}$, which is defined as the net ratio on the surface j of absorbed solar radiation reflected from the surface l (see Fig.4).

$$\gamma_{l,j} = F_{l,j} a_j + \sum_{k=1}^j F_{l,k} \rho_k \gamma_{k,j} \quad (29)$$

$$ADT_{m,j} = TDN_m \sum_{l=1}^L (\delta_{j,l} a_l \cos \theta_l + \rho_l \gamma_{l,j} \cos \theta_l S_l / S_j) \quad (30)$$

$$(\delta_{j,l} = 1 \text{ when } j=l, \delta_{j,l} = 0 \text{ when } j \neq l)$$

Eq.(30) can be rearranged into Eq.(32) by the reciprocal theorem expressed by Eq.(31).

$$a_l S_l \gamma_{l,j} = a_j S_j \gamma_{j,l} \quad (31)$$

$$ADT_{m,j} = a_j \cdot TDN_m \sum_{l=1}^L (\delta_{j,l} + \rho_l \gamma_{j,l} / a_l) \cos \theta_l \quad (32)$$

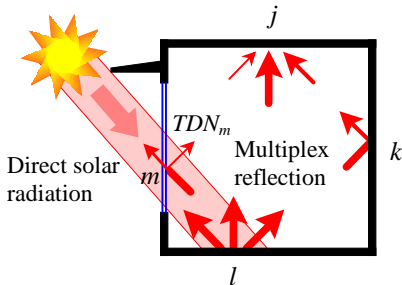


Fig.4 Multiplex reflection of transmitted direct solar radiation

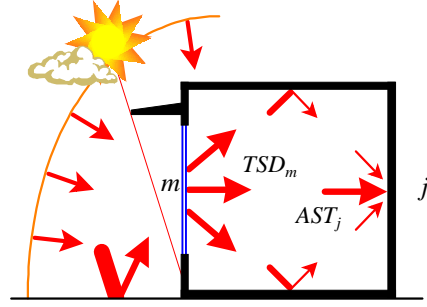


Fig.5 Multiplex reflection of transmitted sky diffuse solar radiation

When ADW_m is the direct absorption of direct solar radiation on window m , the solar absorption ADT_j on the interior surface j is obtained by Eq.(33).

$$ADT_j = \sum_{m=1}^M \left\{ \delta_{j,m} ADW_m + a_j \cdot TDN_m \cdot \sum_{l=1}^L (\delta_{j,l} + \rho_l \gamma_{j,l} / a_l) \cos \theta_l \right\} \quad (33)$$

Regarding sky diffuse solar radiation, when TSD_m is the transmitted sky diffuse solar radiation through the window m and ASW_m is the direct absorption of the sky diffuse solar radiation on window m , the solar absorption AST_j on the interior surface j is obtained by Eq.(34) if TSD_m is assumed to spread equally into the room (see Fig.5).

$$AST_j = \sum_{m=1}^M (\delta_{j,m} ASW_m + a_j \gamma_{j,m} TSD_m / a_m) \quad (34)$$

The short-wave absorption coefficient can be applied to short-wave radiant heat emitted from lights and appliances, etc. If it is assumed that the radiant heat is equally emitted from some parts of ceiling, the absorption amount ASR_j on the surface j can be described by Eq.(35).

$$ASR_j = \sum_{c=1}^C \gamma_{c,j} SI_c S_c / S_j$$

$$= a_j \sum_{c=1}^C \gamma_{j,c} SI_c / a_c \quad (35)$$

where SI_c is the short-wave radiant heat from lights and appliances. Thus the absorption amount NSR_j of the short-wave radiant heat on the surface j is expressed by Eq.(36)

$$NSR_j = ADT_j + AST_j + ASR_j \quad (36)$$

Multi-Layer Window Model

When solar radiation transmits through double-glazing (through 1 to 2 as in Fig.6), the overall transmittance, absorptance and reflectance of the window caused by

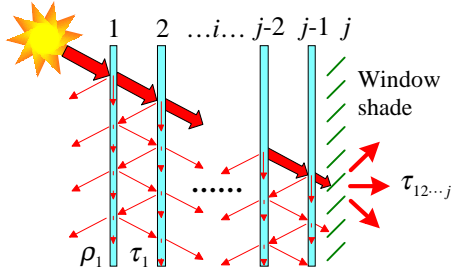


Fig.6 Multi-layer window model

multiple reflections between the glazings can be described by the following infinite series.

$$\begin{aligned} \tau_{12} &= \tau_1\tau_2 + \tau_1\tau_2\rho_1\rho_2 + \tau_1\tau_2\rho_1^2\rho_2^2 + \dots \\ &= \frac{\tau_1\tau_2}{1 - \rho_1\rho_2} \end{aligned} \quad (37)$$

$$\begin{aligned} \alpha_{\bar{1}2} &= \alpha_1(1 + \tau_1\rho_2 + \tau_1\rho_1\rho_2^2 + \dots) \\ &= \alpha_1 \left(1 + \frac{\tau_1\rho_2}{1 - \rho_1\rho_2} \right) \end{aligned} \quad (38)$$

$$\begin{aligned} \alpha_{1\bar{2}} &= \alpha_2\tau_1(1 + \rho_1\rho_2 + \rho_1^2\rho_2^2 + \dots) \\ &= \frac{\alpha_2\tau_1}{1 - \rho_1\rho_2} \end{aligned} \quad (39)$$

$$\begin{aligned} \rho_{12} &= \rho_1 + \tau_1^2\rho_2 + \tau_1^2\rho_1\rho_2^2 + \dots \\ &= \rho_1 + \frac{\tau_1^2\rho_2}{1 - \rho_1\rho_2} \end{aligned} \quad (40)$$

where α_1, ρ_1, τ_1 and α_2, ρ_2, τ_2 are the absorptance, reflectance and transmittance of the glazing layers 1 and 2. $\alpha_{\bar{1}2}$ and $\alpha_{1\bar{2}}$ are the overall absorptance of glazing 1 and 2, respectively. ρ_{12} is the overall reflectance on the side of glazing layer 1 of a double-glazed window.

If the overall transmittance, absorptance and reflectance of a double-glazed window are regarded as the properties of an imaginary single glazing, the equations for triple-glazing can be described as follows.

$$\tau_{123} = \frac{\tau_{12}\tau_3}{1 - \rho_{21}\rho_3} \quad (41)$$

$$\alpha_{1\bar{2}3} = \frac{\alpha_3\tau_{12}}{1 - \rho_{21}\rho_3} \quad (42)$$

$$\left(\rho_{21} = \rho_2 + \frac{\tau_2^2\rho_1}{1 - \rho_1\rho_2} \right)$$

where $\rho_{21} (\neq \rho_{12})$ is the overall reflectance on the side of glazing layer 2 of the double-glazed window.

By regarding the glazing 2-3 of triple-glazing as an imaginary single glazing, the following equations are obtained.

$$\alpha_{\bar{1}23} = \alpha_1 \left(1 + \frac{\tau_1\rho_{23}}{1 - \rho_1\rho_{23}} \right) \quad (43)$$

$$\alpha_{1\bar{2}3} = 1 - \tau_{123} - \rho_{123} - \alpha_{\bar{1}23} - \alpha_{12\bar{3}} \quad (44)$$

$$\text{or } \alpha_{1\bar{2}3} = \alpha_{\bar{1}23} - \alpha_{12\bar{3}} \quad (45)$$

Thus the general equations of overall transmittance, absorptance and reflectance of multi-layer glazing including a window shade can be expressed as follows.

$$\tau_{12...j} = \frac{\tau_{12...j-1}\tau_j}{1 - \rho_{j-1...21}\rho_j} \quad (46)$$

$$\alpha_{12...j} = \frac{\tau_{12...j-1}\alpha_j}{1 - \rho_{j-1...21}\rho_j} \quad (47)$$

$$\left(\rho_{j...21} = \rho_j + \frac{\tau_j^2\rho_{j-1...21}}{1 - \rho_j\rho_{j-1...21}} \right) \quad (48)$$

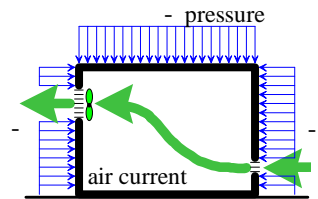
$$\alpha_{12...i...j} = \alpha_{12...i...j} - \alpha_{12...i+1...j} \quad (48)$$

$$\alpha_{\bar{1}2...j} = \alpha_1 \left(1 + \frac{\tau_1\rho_{23...j}}{1 - \rho_1\rho_{23...j}} \right) \quad (49)$$

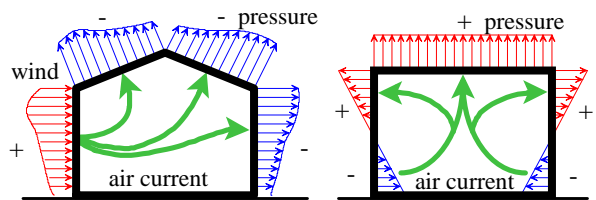
$$\left(\begin{aligned} \alpha_{12...i...j} &= \frac{\tau_{12...i-1}\alpha_{i...j}}{1 - \rho_{i-1...21}\rho_{i...j}} \\ \alpha_{i...j} &= 1 - \tau_{i...j} - \rho_{i...j} \\ \rho_{i...j} &= \rho_i + \frac{\tau_i^2\rho_{i+1...j}}{1 - \rho_i\rho_{i+1...j}} \end{aligned} \right)$$

VENTILATION

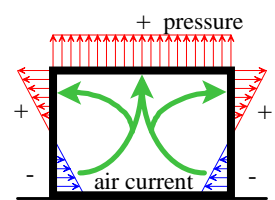
A standard model, called the network airflow model, is used to calculate ventilation quantities of each zone where zones are represented by nodes. Alternatively set constant ventilation quantities in each zones for each hour can also be defined in THERB. Furthermore the dimensionless buoyant airflow model can be also applied to independent ventilated cavities in the walls.



(a) Mechanical Ventilation



(b) Wind forced ventilation

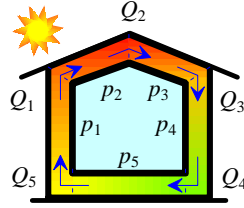


(c) Buoyant ventilation

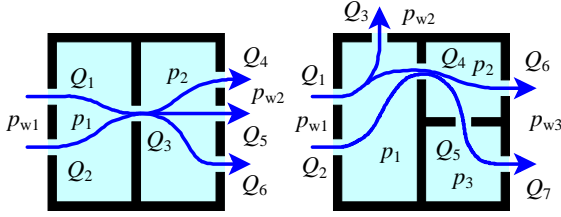
Fig.7 Mechanical or natural ventilation

Network Airflow Model

The network airflow model, which is based on the equations of continuity and airflow quantities for openings and cracks as shown in Eqs.(50) to (52), is solved



(a) Buoyant airflow



(b) Natural or forced ventilation

Fig.8 Network airflow model based on the equations of continuity and airflow quantities

$$\sum_{i=1}^l Q_i = 0 \quad (50)$$

$$Q_i = \alpha_i A_i \sqrt{\frac{2g}{\gamma} |\Delta p_i|} \equiv 4\alpha_i A_i \sqrt{|\Delta p_i|} \quad (51)$$

$$Q_i = a_i l_i \Delta p_i^{1/n} \quad (52)$$

where A is the opening area, Q is the airflow quantity, a is crack constant, g is gravitational constant, l is the length of crack, $n \equiv 1.5$ (constant 1 to 2), Δp is the pressure difference, α is the flow factor and γ is the specific weight of air.

Dimensionless Buoyant Airflow Model in Cavity

Buoyant airflow quantity through a cavity sandwiched between a heating and adiabatic surface as in Fig.9 can be estimated by the equations of continuity, energy and motion described by Eqs.(53) to (55).

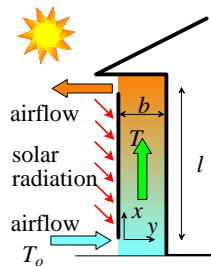


Fig. 9 Wall cavity

$$\frac{\partial u}{\partial x} + \frac{\partial v}{\partial y} = 0 \quad (53)$$

$$\rho c_p u \frac{\partial T}{\partial x} + \rho c_p v \frac{\partial T}{\partial y} = \lambda \frac{\partial^2 T}{\partial y^2} \quad (54)$$

$$u \frac{\partial u}{\partial x} + v \frac{\partial u}{\partial y} = v \frac{\partial^2 u}{\partial y^2} - \frac{1}{\rho} \frac{\partial P_d}{\partial x} + \beta g (T - T_o) \quad (55)$$

$$\left(P_d = p - p_o, \beta = \frac{\rho_o - \rho}{\rho(T - T_o)} \right)$$

Eq.(56) expresses boundary conditions.

$$\left. \begin{aligned} x=0, 0 < y < b: u = \bar{u}, v = 0, T = T_o \\ y=0, x \geq 0: u = 0, v = 0, T = T_w \\ y=b, x \geq 0: u = 0, v = 0, \partial T / \partial y = 0 \\ x=0: P_d = 0 \\ x=l: P_d = 0 \end{aligned} \right\} \quad (56)$$

Eqs.(53) to (56) can be rearranged into the dimensionless equations expressed by Eqs.(58) to (61) by applying the following dimensionless number.

$$\left. \begin{aligned} U = \frac{bu}{vGr}, V = \frac{bv}{v} \\ X = \frac{x}{bGr}, Y = \frac{y}{b} \\ P = \frac{P_d b^2}{\rho v^2 Gr^2}, \Theta = \frac{T - T_o}{T_w - T_o} \\ Gr = \frac{g\beta(T_w - T_o)b^3}{v^2}, Pr = \frac{\mu c_p}{\lambda} \end{aligned} \right\} \quad (57)$$

Equations of continuity, energy and motion are rewritten as follows:

$$\frac{\partial U}{\partial X} + \frac{\partial V}{\partial Y} = 0 \quad (58)$$

$$U \frac{\partial \Theta}{\partial X} + V \frac{\partial \Theta}{\partial Y} = \frac{1}{Pr} \frac{\partial^2 \Theta}{\partial Y^2} \quad (59)$$

$$U \frac{\partial U}{\partial X} + V \frac{\partial U}{\partial Y} = \frac{\partial^2 U}{\partial Y^2} - \frac{\partial P}{\partial X} + \Theta \quad (60)$$

Boundary conditions are represented as follows:

$$\left. \begin{aligned} X=0, 0 < Y < 1: U = Q, V = 0, \Theta = 0 \\ Y=0, X \geq 0: U = 0, V = 0, \Theta = 1 \\ Y=1, X \geq 0: U = 0, V = 0, \partial \Theta / \partial Y = 0 \\ X=0: P = 0 \\ X=L: P = 0 \end{aligned} \right\} \quad (61)$$

where Q (dimensionless buoyant airflow quantity) and L (dimensionless height of a cavity) are defined by Eqs.(62), (63).

$$Q = \frac{b\bar{u}}{vGr} = \int_0^1 U dY \quad (62)$$

$$L = \frac{l}{bGr} \quad (63)$$

In the case difference coordinates are used as in Fig.10, the value of Q can be calculated by Eq.(64) on the basis of Simpson's law.

$$Q = \frac{\Delta Y}{3} \left(4 \sum_{j=1}^{(K-1)/2} U_{m+1,2j} + 2 \sum_{j=1}^{(K-3)/2} U_{m+1,2j+1} \right) \quad (64)$$

If Q and Pr are given as initial conditions, the distributions of pressure, velocity and temperature can

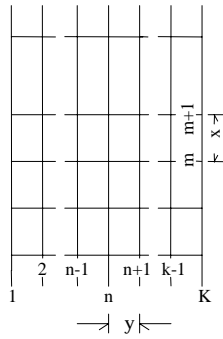


Fig.10 Difference coordinates

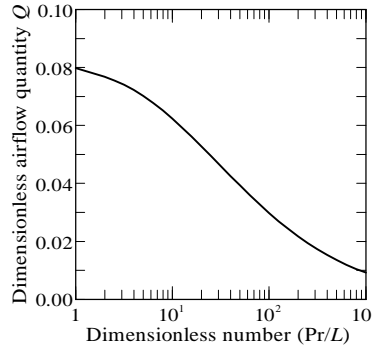


Fig.11 Correlation between Q and Pr/L

be solved from Eqs.(58) to (60) for every height level by convergence calculation as a function of Q , which is obtained from Eq.(64), on the basis of the boundary conditions. When P becomes 0, the dimensionless height L is obtained and then the relationship of Pr/L (revised Rayleigh number) to Q is identified as in Fig.11.

CONCLUSIONS

The theoretical models of heat transfer used in THERB (the simulation software of the thermal environment of residential buildings) are outlined and the following prominent features of the models are highlighted.

- 1) Calculation time and storage capacity for transient thermal conduction of multi-layer walls in the time-discrete domain are decreased by making use of the successive transition method and the accuracy of conductive heat is increased by applying the trapezoid hold function which can adjust itself to the time-discrete domain.
- 2) Dimensionless equations, which are derived from the profile method for boundary layer or defined from experimental findings according to natural or forced convection, are used to calculate convective heat transfer coefficients for every part of buildings.
- 3) The long-wave and short-wave absorption coefficients make it possible to simulate the net absorption of radiant heat and transmitted solar radiation as a consequence of multiplex reflection among interior surfaces of buildings. Furthermore the absorption coefficients are applicable to radiant heat emitted from lights, appliances and human bodies, etc.
- 4) A multi-layer window model, which defines the overall transmittance, absorptance and reflectance of solar radiation as an infinite series, is proposed.
- 5) A network airflow model is used to calculate ventilation quantities in each zone where each zone is represented by nodes. Furthermore, the

dimensionless buoyant airflow model derived from this network model is applicable to independent ventilated wall cavities.

REFERENCES

- [1] Watanabe T., Ozaki A., et al. (1985), 'Practical Methods for Calculating Unsteady-State Heat Conduction of Multi-Layer Walls Based on Pulse Transfer Function', *Journal of Architecture, Planning and Environmental Engineering*, Architectural Institute of Japan, No.391, 8-19
- [2] Stephenson D.G. and Mitalas G.P. (1967), 'Cooling Load Calculation by Thermal Response Factor Method', *ASHRAE Transactions*, Vol.73-I
- [3] Urano Y. and Watanabe T. (1981), 'Analysis of Conductive Heat Transfer of Multi-Layer Wall by State Transition Determinant - Part 1', *Journal of Architecture, Planning and Environmental Engineering*, Architectural Institute of Japan, No.305, 97-111
- [4] Pipes L.A. (1957), 'Matrix Analysis of Heat Transfer Problems', *Journal of Franklin Institute*, Vol.263, No.3
- [5] Nishikawa K. and Fujita Y. (1988), *Heat Transfer*, Rikougakusha
- [6] Ozaki A., Watanabe T., et al. (1990), 'Heat and Mass Transfer at Outside Surface of Buildings - Wind Tunnel Tests of Heat and Mass Transfer on Horizontal Surfaces', *Journal of Architecture, Planning and Environmental Engineering*, Architectural Institute of Japan, No.407, 11-25
- [7] Fujii W. and Imura H. (1972), 'Natural Convection Heat Transfer from a Plate with Arbitrary Inclination', *Int. J. Heat Mass Transfer*, Vol.15, 755-767
- [8] Perez R., et al. (1990), 'Modeling Daylight Availability and Irradiance Components from Direct and Global Irradiance', *Solar Energy*, Vol.44, No.5, 271-289
- [9] Ono K., Ozaki A., et al. (1996), 'Calculation of Direct Solar Heat Gain through Glazing - Successive Incident Angle Method and Solar Shading Coefficient Method', *Fukuoka University Review of Technological Sciences*, No.58, 67-75
- [10] Ozaki A., Watanabe T., et al. (1997), 'Analysis of Draft Quantity through Ventilated Air Space', *Proc. of the 14th International Conference on Passive and Low Energy Architecture*, Vol.2, 33-38
- [11] ASHRAE (1972), *ASHRAE Handbook of Fundamentals*, 425-440
- [12] July E.I. (1958), 'Sampled-Data Control System', *John Wiley & Sons*
- [13] Urano Y. and Watanabe T. (1982), 'Analysis of Conductive Heat Transfer of Multi-Layer Wall by State Transition Determinant - Part 2', *Journal of Architecture, Planning and Environmental Engineering*, Architectural Institute of Japan, No.311, 57-66
- [14] Gebhart, B. (1959), 'A New Method for Calculating Radiant Exchanges', *ASHRAE Transactions*, Vol.65